Annals of Operations Research
https://doi.org/10.1007/s10479-026-07166-1

ORIGINAL RESEARCH

Dynamic analysis of degradation thresholds for sustainable environmental management

Fabio Lamantia[1] · **Davide Radi**[2,3] · **Iryna Sushko**[2,4]

Received: 29 April 2025 / Accepted: 12 March 2026

Abstract
We examine environmental protection in an oligopolistic setting in which a Pigouvian pollution tax is levied whenever environmental degradation exceeds a certain threshold set by a regulator. This threshold mechanism defines two scenarios, one with low environmental degradation in which firms do not internalize pollution, and one with high degradation in which firms are involved not only in production activities but also in abatement to ease the burden of the environmental tax. The purpose of this paper is to examine how the periodic dynamics of environmental degradation, described by a *Lorenz* map, are influenced by the main policy parameters. Regarding policy implications, we show how to construct a careful alignment between the border of the no-tax area and the level of taxation, which is crucial for reducing environmental degradation and avoiding fluctuations.

Keywords Thresholds · Pigouvian Tax · Environmental protection · Complex Economic Systems · Economic Dynamics

JEL Classification C62 · C73 · D21 · D43

1 Introduction

Environmental protection is a major concern in today's world, as economic activity significantly contributes to pollution. Pollution is a typical example of a *negative externality*: the main costs of pollution (say, health issues and damages to the environment) do not typically fall on the polluters but on society in general. The main tools to alleviate pollution can be split into two main categories: *command-and-control* instruments and *market-based* instruments.

✉ Davide Radi
davide.radi@unicatt.it

1 Department of Economics and Business, University of Catania, Catania, Italy

2 DiMSEFA, Catholic University of Sacred Heart, Milan, Italy

3 Department of Finance, VŠB - Technical University of Ostrava, Ostrava, Czech Republic

4 Institute of Mathematics, NAS of Ukraine, Kyiv, Ukraine

Published online: 07 April 2026

Command-and-control instruments rely on mandatory standards, such as prohibitions on the use of certain substances or technologies, or emission thresholds set by regulators, which directly prescribe the actions firms must take. These thresholds represent boundaries on emissions and pollution levels, allowing industries and other institutions to operate within environmentally secure ranges, see Bennett et al. (2008). In some cases, thresholds are set not to go higher than concentrations of pollution deemed to be dangerous to health; in other cases, thresholds are differentiated in reaction to the condition of the environment. For instance, water quality standards might be differentiated for seasonal fluctuations in water consumption and flow, Chidiac et al. (2023). Generally, agencies set thresholds in line with national or international standards. Examples in question pertain to the activities of the European Environment Agency (EEA) or the United States Environmental Protection Agency (EPA).[1] Such agencies report on the environment to help in sustainable development and improve environmental standards. The EPA, for instance, defines the *National Ambient Air Quality Standards* (NAAQS) by setting thresholds for pollutants such as *carbon monoxide*, *lead*, *nitrogen dioxide*, *ozone*, *particulate matter*, and *sulfur dioxide*.[2] They are thresholds put to safeguard public health and the environment through the lowering of the concentration of pollutants in the air. Even though there is no standard set worldwide, most countries use similar thresholds to safeguard the environment (Bennett et al., 2008). Imposing a pollution threshold, however, entails costs for both the industrial sector and society. Therefore, regulators must assess the associated costs, such as monitoring and compliance costs, and set the threshold on the basis of a cost–benefit analysis. Economic models, such as the one developed in this paper, help policymakers make informed decisions.

In contrast, market-based instruments use taxes or tradable permits to shape firms' incentives, letting the market determine the most efficient way to reduce pollution, see Jørgensen et al. (2010). Such measures are necessary because pollution, as a negative externality, represents a classic case of market failure: it imposes social costs that are not internalized in the market prices of goods and services. Pigouvian taxes are a common market-based instrument to force polluters to internalize such externalities, see Carlsson (2000), although their effectiveness is sometimes questioned, see Manta et al. (2023). A prominent example of this approach is *carbon pricing*, a regulatory policy designed to make polluters bear part of the social cost of emissions. This form of taxation is levied on the carbon content of fossil fuels, thereby assigning a price to carbon emissions. Another more sophisticated market-based approach is applying *cap and trade* systems, whereby the regulator puts a cap (restriction) on emissions, and firms can sell and purchase certificates to emit a certain amount of pollutants. The EU Emissions Trading System (EU ETS) is an example of such a system. Recently, the interest in understanding how market-rule compatible mechanisms can facilitate the adoption of sustainable behavior has grown, see Ulph (1996); van der Ploeg and de Zeeuw (1992); Marsiglio and Tolotti (2024); Buccella et al. (2024a) and references therein. Understanding their effects over time is a central focus of research, as also emphasized in He et al. (2023). A contribution in this direction is provided by Buccella et al. (2024b), where the *abatement game* introduced in Buccella et al. (2021) is extended to account for oligopolistic competition among heterogeneous firms. The analysis focuses on optimal tax regulation and the efficiency of market outcomes, also from a dynamic perspective. A broad review of the literature on this

[1] See https://www.eea.europa.eu/en/about/policy-corner-eu-policies-we-support and https://www.epa.gov/environmental-topics

[2] See https://www.who.int/teams/environment-climate-change-and-health/air-quality-and-health/health-impacts/types-of-pollutants

topic, with particular emphasis on the role of environmental taxation, can instead be found in Jørgensen et al. (2010).

Regarding empirical assessment of their effectiveness, Ma et al. (2024) provide evidence that different forms of environmental regulation–command-based, market-oriented, and voluntary–stimulate technological innovation, with heterogeneous and short-run effects across firms. Their findings confirm that regulatory interventions can induce shifts in firms' behavior, consistent with the regime-switching mechanisms captured by a threshold framework. Nevertheless, each regulatory scheme has its own side effects. For instance, a market-oriented policy based on a green tax may jeopardize industrial competitiveness, even when pollution levels are under control and below safeguard thresholds. Conversely, command-based green policies can create market oscillations. Recent empirical research supports the existence of recurrent (quasi-cyclical) dynamics in environmental systems arising from the interaction between regulatory pressure and firms' strategic responses. Firm-level evidence in Feng et al. (2025) shows self-reinforcing feedbacks among environmental regulation, technological innovation, and emissions, producing sequences of adjustments over time consistent with oscillatory behavior.

To address the limitations of these two green policy approaches while retaining their benefits, we propose a hybrid regulatory scheme that combines a threshold-based command-and-control rule with a Pigouvian tax once the threshold is exceeded. This allows us to study how the interaction between these two regulatory instruments shapes the dynamics of environmental degradation and may allow to overcome the side effects of both. As a first attempt to investigate this hybrid approach in a dynamic context, we propose a much simpler industrial setup than Buccella et al. (2024b). The industry is served by one (monopolist) or a finite number of homogeneous firms (oligopolists). Based on economic, social, and political considerations, the regulator sets a threshold level of pollution beyond which environmental degradation requires strong regulatory measures. Specifically, below the threshold, there is a good perception of environmental quality, and no restriction is imposed on the industry; in contrast, above the threshold level, a Pigouvian pollution tax is imposed. Above the environmental threshold, each firm can take emission abatement measures and pays this tax based on net emissions to the environment. In other words, following Segerson (1988), we assume a combination of a command-and-control instrument (an environmental threshold) with a market-based instrument (a Pigouvian tax). Our focus, from this point of view, is more on the possible periodic dynamics that can be obtained from a simple on-off mechanism on the imposition of stricter rules if certain thresholds of environmental degradation are crossed. Despite the simplicity of the rule, our interest is precisely in studying the possible non-convergence dynamics that follow from these policies. In particular, we study the bifurcations through which these oscillatory dynamics arise, as this analysis provides policy-relevant insights on how to prevent or mitigate them. To obtain analytical results and keep the setup as simple as possible, we assume an economic context characterized by linear demands and quadratic abatement costs, which are a common assumption in the literature, see Buccella et al. (2024b) and Ulph (1996). The dynamics of environmental degradation can be modelled through a discontinuous map of the *Lorenz* type, that is, a one-dimensional piecewise monotone map with one discontinuity point, whose branches are defined by linear functions. The dynamics of these maps have been extensively studied, see Avrutin et al. (2019), with basic results related to attractors and bifurcations useful for model dynamics. For this map, we present a complete analysis focusing on the most relevant policy parameters, given by the threshold level of environmental degradation that triggers additional measures and the amount of the

tax. The purpose of maintaining an extremely simple economic structure also relates to our desire to exhibit the possible dynamics of environmental degradation that can be achieved even with an extremely simplified economic and environmental system. Here we do not focus on the *optimality* of the threshold, which, as we have seen, can be established by varied considerations through cost-benefit analysis or from a sustainability perspective. However, we seek to clarify how major policy choices, in terms of threshold and amount of taxation, contribute to the overall dynamics of environmental degradation. This is also a first step in the analysis of a more sophisticated system in which multiple thresholds for different pollutants can be imposed.

Our main findings regarding policy implications indicate that there is a threshold level for the no-tax area that makes taxation ineffective. We quantify this threshold analytically. Below this threshold, an increase in taxation can lead to a reduction in environmental degradation. However, if taxation is not properly aligned with the border of the no-tax region, an increase in taxation may result in fluctuations that can, on average, increase environmental degradation. The key takeaway is that the border of the no-tax area and the level of taxation need to be carefully aligned to achieve a reduction in environmental degradation and avoid persistent oscillatory dynamics.

The paper is structured as follows. Section 2 presents the economic setup with production and abatement efforts. The dynamics of environmental degradation is modelled through a discontinuous map, which arises because of the environmental threshold level above which a stricter regulation is imposed. Section 3 presents a complete dynamic characterization of the map, focusing in particular on the periodic attractors induced by its discontinuity. Section 4 draws upon the analysis of the map to present the main economic insights and policy implications of the presence of an environmental threshold of taxation. Section 5 concludes and presents some discussions on further developments of the model.

2 Model

We start by briefly describing the economic setup for industrial activity. A homogeneous good is sold in the market at price:

$$P(Q) = a - Q \tag{1}$$

where a is the reservation price and Q is aggregate supply. Assume $n \geq 1$ firms serve the market. When $n = 1$, a monopolist operates, whereas the market is oligopolistic for a fixed $n > 1$. We denote by q_i the production sold in the market by firm i, with total industry production $\sum_{i=1}^{n} q_i = Q$. A by-product of production is pollution, which firms can reduce through abatement efforts, see van der Ploeg and de Zeeuw (1992) and Ulph (1996). This activity is costly, and, analogously to Ulph (1996) and Buccella et al. (2021), firm i reduces its emissions by ω_i, incurring abatement costs given by

$$C_i(\omega_i) = \gamma_i \frac{\omega_i^2}{2} \tag{2}$$

where γ_i measures the inefficiency of firm i's abatement efforts. This is the simplest functional form for an abatement cost function that captures increasing marginal costs of abatement, a

feature expected to arise in many contexts. Indeed, achieving each additional unit of pollution reduction typically requires more advanced technologies, greater effort, or the adoption of less efficient production processes.[3] As for production, we assume linear production costs and, without loss of generality, we set a marginal cost equal to zero.

As said, pollution is a by-product of the industry production process. The environmental degradation caused by production is modelled through a *damage function*, which we assume is linear in net emissions, that is

$$D\left(q_1, \ldots, q_n, \omega_1, \ldots, \omega_n\right) = \sum_{i=1}^{n} \left(\delta_i q_i - \omega_i\right) \tag{3}$$

where δ_i denotes the units of pollution for a unit of production, so that $\delta_i q_i$ represents gross emissions from the production of good by firm i (after some appropriate choice of units). We assume that $\omega_i \in [0, \delta_i q_i]$, that is firm i cannot abate more than its emissions. Environmental abatement increases total costs but reduces emissions. Emissions by all firms define a composite pollution index, which is dynamically updated according to biodegradation and pollution released over time. This index, which we refer to as the *level of environmental degradation* at time t, is denoted by N_t. The environment can abate a part of pollution at a constant rate μ for a unit of time. The dynamics of environmental degradation in discrete time can be modelled by a map of the form

$$N_{t+1} = (1 - \mu) N_t + D\left(q_{1,t}, \ldots, q_{n,t}, \omega_{1,t}, \ldots, \omega_{n,t}\right) \tag{4}$$

where $q_{i,t}$ and $\omega_{i,t}$ are the levels of production and abatement of firm $i, i = 1, \ldots, n$, at time t.[4]

Following Segerson (1988), the regulator fixes a threshold level of natural degradation $\tilde{N}$, above which a tax on the net emission is imposed. When natural degradation is low, namely $N_t < \tilde{N}$, firms set their production plans knowing that the regulator will not impose taxes on emissions.[5] Therefore, profit-maximizing firms will not exert abatement efforts ($\omega_i = 0$). When $n = 1$, the monopolist maximizes its profit, whereas when $n > 1$, firms set their production at a Cournot-Nash level. Hence, firm i solves the problem

$$q_i^* = \underset{q_i \in [0, +\infty)}{\arg\max}\ \pi_i\left(q_i\right) = \underset{q_i \in [0, +\infty)}{\arg\max} \left(a - q_i - \sum_{j \neq i} q_j\right) q_i . \tag{5}$$

[3] Note that an alternative cost function with constant marginal costs would imply stronger incentives for abatement, as pollution reduction would be relatively cheaper at the margin. Therefore, the current formulation can also be interpreted as a worst-case benchmark relative to the linear specification. Moreover, the assumption of constant marginal abatement costs restricts the adjustment of the tax rate to two distinct regimes: values at which firms find it optimal to abate fully, in which case the map describing the model's dynamics remains of the same type, and values at which firms choose not to abate at all, in which case the map is linear.

[4] Following, for instance, La Torre et al. (2025), a random additive term could be introduced into the pollution dynamics (4) to account for the impact of natural disasters, such as volcanic eruptions, on environmental quality. This extension is not considered here and is left for future work.

[5] Note that the threshold-based command-and-control policy we consider is backward-looking: the current level of environmental damage results from past production, and, if the threshold is exceeded, a pollution tax affects the current optimal level of production, which in turn influences the environmental quality observed at the beginning of the next period. Consequently, myopic, one-period profit-maximizing firms cannot strategically avoid the threshold by adjusting current production.

Then, under homogeneity, that is $q_i^\star = q^\star, \forall i = 1, \ldots, n$, each firm will produce the Cournot-Nash quantity $q^* = \frac{a}{1+n}$, which coincides with the monopoly quantity when $n = 1$. When firms are homogeneous also for emissions, that is $\delta_i = \delta, \forall i = 1, ..., n$, individual net emissions are given by $\delta q^* = \frac{a\delta}{1+n}$. Summing up for all firms, total net emissions of the industry are given by $\frac{a\delta n}{1+n}$ whenever $N_t < \tilde{N}$.

Now assume that $N_t \geq \tilde{N}$. The regulator will then set a tax on firms' net emissions to reduce environmental degradation. In this case, the profit function of firm i becomes

$$\tilde{q}_i = \underset{q_i \in [0,+\infty)}{\arg\max}\ \tilde{\pi}_i\left(q_i, \omega_i; T\right) = \underset{q_i \in [0,+\infty)}{\arg\max} \left(a - q_i - \sum_{j \neq i} q_j\right) q_i - \gamma_i \frac{\omega_i^2}{2} - T(\delta_i q_i - \omega_i). \tag{6}$$

where the term $T(\delta_i q_i - \omega_i)$ represents the taxation on firm's i net emissions when $N_t \geq \tilde{N}$. The solution concept we adopt is that of subgame perfect Nash equilibrium (SPNE): each firm optimizes in a two-stage fashion by setting optimal abatement and production plans. The last decision is that of production, where each firm selects $\tilde{q}_i = \max\left[0, \frac{a-\delta_i T}{1+n}\right]$. Hence, optimal production $\tilde{q}_i$ is positive whenever $T < \hat{T} = \frac{a}{\delta_i}$, see Buccella et al. (2024b) for a similar specification. At the first stage of the game, each firm selects optimal emissions. Assuming homogeneity across firms hereafter–namely, identical technologies, such that $\delta_i = \delta$, and identical abatement cost functions, such that $\gamma_i = \gamma$–optimal abatement levels are defined as follows:

$$\tilde{\omega} = \underset{\omega \in [0, \delta\tilde{q}]}{\arg\max}\ \tilde{\pi}\left(\tilde{q}, \omega; T\right) = \underset{\omega \in [0, \delta\tilde{q}]}{\arg\max} \frac{(a - \delta T)^2}{(n+1)^2} + T\omega - \gamma \frac{\omega^2}{2} = \frac{T}{\gamma}. \tag{7}$$

Employing the optimal production and abatement levels, we identify two threshold values of the environmental tax, $\bar{T}$ and $\hat{T}$. The first threshold,

$$\bar{T} = \frac{a\delta}{\delta^2 + \frac{1+n}{\gamma}}, \tag{8}$$

represents the minimum tax level at which a firm's optimal emissions drop to zero. The second threshold, previously introduced,

$$\hat{T} = \frac{a}{\delta}, \tag{9}$$

corresponds to the tax level above which a firm optimally chooses to cease production. Then, individual net emissions are given by

$$\delta\tilde{q} - \tilde{\omega} = \begin{cases} \frac{\delta(a-\delta T)}{1+n} - \frac{T}{\gamma} & \text{if} \quad T \leq \bar{T} \\ 0 & \text{if} \quad \bar{T} < T \end{cases} \tag{10}$$

Summing up, if $N_t < \tilde{N}$, the environmental damage is $D = \frac{an\delta}{1+n}$. Instead, for $N_t > \tilde{N}$, the environmental damage is $D = n\left(\delta\tilde{q} - \tilde{\omega}\right)$. Hence, the damage function (3) assumes the following form:

$$D = \begin{cases} \frac{na\delta}{1+n} & \text{if} \quad 0 < N_t < \tilde{N} \\ n \max\left[0, \frac{\delta(a-\delta T)}{1+n} - \frac{T}{\gamma}\right] & \text{if} \quad N_t \geq \tilde{N} \end{cases} \tag{11}$$

Following the construction of the model, the derivation of firms' optimal strategies, and the specification of the damage function, a first policy implication arises, as highlighted in the following proposition.

Proposition 1 *Optimal productions and profits decrease in T, for $T \in \left[0, \hat{T}\right)$. For $T < \bar{T}$, environmental damage remains positive. For $T \in \left[\bar{T}, \hat{T}\right)$, environmental damage is zero while optimal production remains positive. For $T > \hat{T}$, environmental damage, optimal production, and profits are all zero. If the policymaker aims to reduce environmental damage while preserving economic activity in the industry, taxation should never exceed $\bar{T}$.*

Proof of Proposition 1 Note that the solution to problem (6) is either a linear function of T with negative coefficient $-\delta/(1+n)$ or zero. Therefore, optimal production declines as the tax increases, or remains constant at zero. Hence, optimal profit does so as well, being increasing in the optimal level of production. Solving for the value of T for which the solution of problem (6) becomes zero, namely $\tilde{q} = \max\left\{0, \frac{a-\delta T}{1+n}\right\}$, yields the threshold $\hat{T}$. Analogously, solving for the value of T that sets the solution of problem (7) equal to zero yields the threshold $\bar{T}$. Straightforward algebra shows that $\bar{T} < \hat{T}$. Assuming that the policymaker aims to balance environmental damage with the preservation of economic activity, the policy implication follows directly from the above arguments. □

Proposition 1 provides a first policy guideline: the tax rate T should not be set above $\bar{T}$. Indeed, when the regulator sets taxation equal to $\bar{T}$, firms no longer find it profitable to emit. Any further increase in taxation would only reduce production, without generating additional environmental benefits. Since we assume that the regulator seeks to reduce environmental damage while preserving economic activity, we henceforth restrict our attention to the case $T < \bar{T}$.

The dynamics of environmental degradation when $T < \bar{T}$ can be written as a piecewise-linear discontinuous map (increasing-increasing) of the form:

$$N_{t+1} = \begin{cases} N_t\,(1-\mu) + \frac{na\delta}{n+1} & \text{if} \quad 0 < N_t < \tilde{N} \\ N_t\,(1-\mu) + \frac{na\delta}{n+1} - nT\left(\frac{1}{\gamma} + \frac{\delta^2}{n+1}\right) & \text{if} \quad N_t \geq \tilde{N} \end{cases} \tag{12}$$

where μ is the natural abatement rate for a unit of time of the environmental degradation.

In the following, we set

$$A = 1-\mu \in [0,1]\,; \qquad B = \frac{na\delta}{1+n} \in (0,+\infty)\,; \qquad C = -Tn\left[\frac{1}{\gamma} + \frac{\delta^2}{1+n}\right] \in [-B, 0] \tag{13}$$

The aggregate parameter A captures the natural rate of pollution absorption, B measures pollution generated by production in the absence of abatement activities, and C denotes the level of optimal abatement induced by taxation. Hence, $C \geq -B$, as abatement cannot exceed

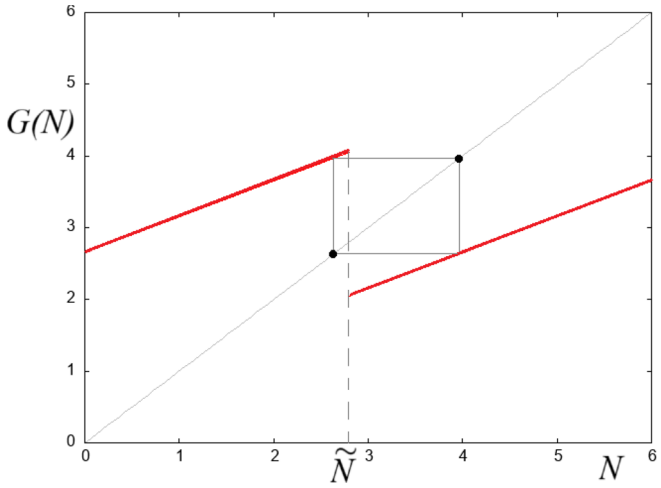

Fig. 1 Map G given in (14) for $\tilde{N} = 2.8, n = 7, a = 7.3, \mu = 0.5, \delta = 0.415, T = 0.7, \gamma = 1$. Any trajectory of the map G converges to the 2-cycle

pollution. Using these aggregate parameters, we rewrite (12) as follows:

$$G: \quad N_{t+1} = \begin{cases} AN_t + B & \text{if} \quad 0 < N_t < \tilde{N} \\ AN_t + B + C & \text{if} \quad N_t \geq \tilde{N} \end{cases} \tag{14}$$

with $\tilde{N} \in [0, +\infty)$.

In the following, we present a complete analysis of the map G and then we study the influence of the policy parameters C and $\tilde{N}$ on the dynamics of environmental degradation.

3 Dynamics

This section summarizes the main properties of the proposed model by presenting a complete characterization of the dynamics. Let us first make a change of the variable, $x_t = N_t/B$, scaling out parameter B, so that map in (14) becomes the following one, denoted F:

$$F: \quad x_{t+1} = \begin{cases} F_L(x_t) = Ax_t + 1 & \text{if} \quad 0 < x_t < \tilde{n} \\ F_R(x_t) = Ax_t + 1 + c & \text{if} \quad x_t \geq \tilde{n} \end{cases} \tag{15}$$

where $\tilde{n} = \tilde{N}/B$ and $c = C/B$. Since it has to be $C \in [-B, 0]$ (see (13)), for the parameter c we have $c \in [-1, 0]$. In (15), the symbols L and R refer to the left and right partitions (intervals) separated by the discontinuity point $x = \tilde{n}$, that is, $L = [0, \tilde{n})$ and $R = [\tilde{n}, +\infty)$.

According to the change of variables adopted, the state variable x and the parameters c and $\tilde{n}$ are expressed in units of pollution generated by production in the absence of abatement;

in this formulation, x denotes environmental degradation, c the abatement level, and $\tilde{n}$ the threshold level.

The global dynamics of the map F is investigated in the following. Before, however, we present some preliminary results that offer policy implications and help to better interpret the technical findings that follow. In the region below the threshold, that is, for $x < \tilde{n}$, the tax does not apply and firms do not undertake any abatement activity. This corresponds to a region where the level of environmental degradation is considered tolerable by the policymaker, or at least not severe enough to require fiscal intervention to contain it. Based on production and the associated pollution level, this region admits the equilibrium

$$L^* = \frac{1}{1-A}. \tag{16}$$

By reducing $\tilde{n}$ to the point where $\tilde{n} < L^*$, L^* is no longer an equilibrium of the model. Furthermore, the model does not admit any equilibrium as long as $R^* < \tilde{n} < L^*$, where

$$R^* = \frac{1+c}{1-A}. \tag{17}$$

As we will see in the following, a threshold level $\tilde{n} \in (R^*, L^*)$ is associated with persistent fluctuations, and the types of behaviors that may arise are discussed in the following.

By further reducing the threshold for fiscal intervention so that $\tilde{n} < R^*$, we enter a region in which a unique equilibrium exists, namely R^*. In this case, pollution taxation induces firms to undertake abatement activities optimally, and the resulting level of environmental damage reaches its minimum attainable value. Indeed, as we will show in the following, the long-run environmental damage is always confined in the range $\left[R^*, L^*\right]$.

Note that increasing taxation, i.e., decreasing c, lowers the lower bound R^*, while L^* remains unchanged. Consequently, the invariant set within which fluctuations occur becomes wider. This implies that, whenever no equilibrium exists, the system may exhibit persistent fluctuations of greater amplitude when an equilibrium cannot be reached.

As discussed, the model exhibits different dynamic regimes. Identifying these regimes is essential for designing an effective tuning of the proposed green policy, and this requires an examination of the model's bifurcations. Therefore, given this brief interpretation of the possible scenarios, the remainder of this section is devoted to a detailed global analysis of the map F, which belongs to a well-known class of *Lorenz maps* which are one-dimensional discontinuous piecewise monotone maps with one discontinuity point (see Rand (1978); Keener (1980); Homburg (1996); Berry and Mestel (1991); Gardini et al. (2010); Avrutin et al. (2019), to cite a few). Many researchers from various theoretical and applied fields have studied Lorenz maps from different perspectives, and today the dynamics of these maps has been described in great detail. The map F is the simplest representative of the class of Lorenz maps, since its branches are defined by linear functions. Below we recall in short some basic results related to the attractors of the map F and their bifurcations (see Avrutin et al. (2019) for details), useful for the understanding dynamics of the model.

- Given that the functions F_L and F_R have the same positive slope which is less than 1, $0 < A < 1$, it immediately follows that map F cannot have repelling cycles and, thus, chaos is also not possible.

- The fixed point $L^* = 1/(1-A)$ of the map F_L is actual for map F if $L^* < \tilde{n}$, and the fixed point $R^* = (1+c)/(1-A)$ of the map F_R is actual for map F if $R^* > \tilde{n}$. Here we assume that $A \neq 1$; for $A = 1$, we have that the fixed points of both maps are at infinity. If the fixed point L^* or R^* exists, it is globally attracting. If $R^* < \tilde{n} < L^*$, then both fixed points are virtual for F.
- The equalities $L^* = \tilde{n}$ and $R^* = \tilde{n}$, leading to

$$\eta_L : \quad \tilde{n} = \frac{1}{1-A} \tag{18}$$

$$\eta_R : \quad \tilde{n} = \frac{1+c}{1-A} \tag{19}$$

  respectively, define *border collision bifurcation*[6] boundaries of the existence regions of the corresponding fixed points in the parameter space of the map F.
- Map F cannot have two coexisting attracting fixed points, since for their existence it has to be $L^* < \tilde{n} < R^*$, and thus, $L^* < R^*$, while for $-1 < c < 0$, it holds $L^* > R^*$.
- For $R^* < \tilde{n} < L^*$, map F belongs to a class of *gap maps*: there exists an absorbing interval $I = [F_R(\tilde{n}), F_L(\tilde{n})]$, and within this interval there is a 'gap', which is the interval $Z = (F_R(F_L(\tilde{n})), F_L(F_R(\tilde{n})))$. Since points of Z have no preimages in I, an attractor of the map F can have points neither in Z, nor in its images.
- A unique attractor of a gap map and, in particular, map F, is either an *attracting cycle* (in a generic case) or a *Cantor set attractor* (in a non generic case). In fact, the rotation number[7], say ρ, which is the same for any point of the absorbing interval I, can either be rational or irrational. If ρ is a rational number, $\rho = k/m$, then the ω-limit set of any trajectory is an attracting cycle, while if ρ is irrational, then the ω-limit set of any trajectory is a Cantor set attractor (a closure of quasiperiodic trajectories).

Now let us comment on the *bifurcation structure* of the parameter space of the map F. It is well-known that in the parameter space of a gap map, periodicity regions related to attracting cycles of different periods are organized in the so-called *period-adding structure* (see e.g., Keener (1980); Homburg (1996); Gardini et al. (2010); Avrutin et al. (2010)).

In Fig. 2(a), the period-adding structure is shown for map F in the $(c, \tilde{n})$-parameter plane for fixed $A = 0.5$. Note that for the parameter values as in Fig. 1, we have that $B \approx 2.6508$, $C \approx -1.9385$, so that $c \approx -0.7313$, $\tilde{n} \approx 1.0563$. One can see that parameter point $(c, \tilde{n}) = (-0.7313, 1.0563)$ (marked by a black dot in Fig. 2(a)) belongs to the periodicity region related to an attracting 2-cycle.

Note also that in the case presented in Fig. 2(a), the border-collision bifurcation boundaries η_L and η_R of the existence regions of the fixed points L^* and R^* are defined by $\tilde{n} = 2$ and $\tilde{n} = 2(1+c)$ (see (18) and (19), respectively). An intersection point of these boundaries, $(c, \tilde{n}) = (0, 2)$, is a codimension-two border-collision bifurcation point (often called the

[6] This term, introduced in Nusse and Yorke (1992), denotes a qualitative change in the dynamics of a piecewise smooth map occurring when its invariant set collides with a border separating different definition regions of the map.

[7] The rotation number of the map F can be defined as $\rho(x) = \lim_{n\to\infty} \frac{1}{n} \sum_{j=0}^{j=n} \kappa((F^j(x)))$, where $\kappa(x) = 1$ in $x \in L$ and $\kappa(x) = 0$ in $x \in R$, see e.g., Keener (1980). The rotation number of an m-cycle can be defined in a simpler way: it is an irreducible fraction $\rho = k/m$, where m is the period of the cycle and k is the number of points in one partition, e.g. in the partition L.

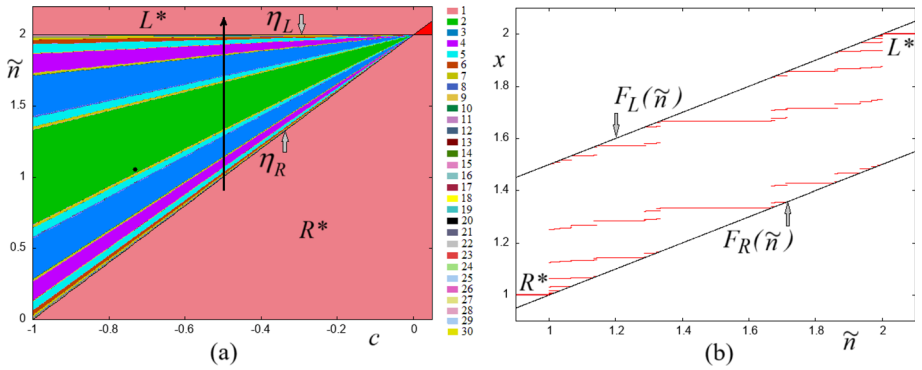

Fig. 2 In **(a)**, two-dimensional bifurcation diagram of the map F given in (15) in the $(c, \tilde{n})$-parameter plane for fixed $A = 0.5$. Different colors are associated with attracting cycles of different periods (see the middle panel for the correspondence between colors and periods). In **(b)**, one-dimensional bifurcation diagram related to the crossection of the bifurcation structure shown in **(a)** along the vertical arrow. Here $x = F_L(\tilde{n})$ and $x = F_R(\tilde{n})$ are the boundaries of the absorbing interval I

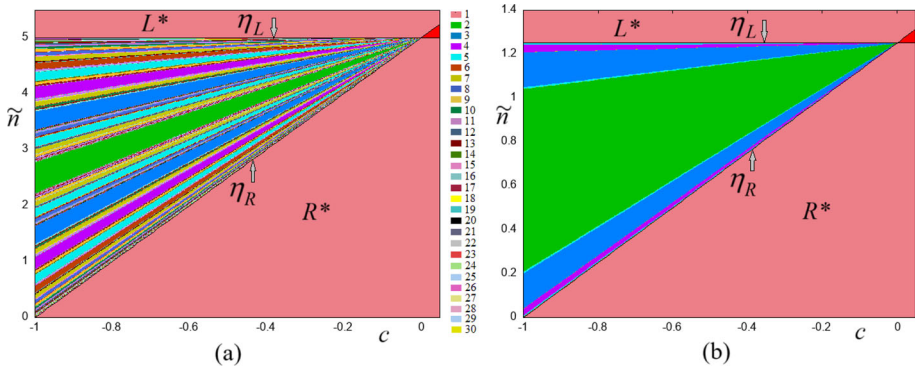

Fig. 3 Two-dimensional bifurcation diagram of the map F given in (15) in the $(c, \tilde{n})$-parameter plane for fixed $A = 0.8$ in **(a)**, and $A = 0.2$ in **(b)**

organizing center) at which $L^* = R^*$ and map F is continuous. Using the theorem proved in Gardini et al. (2014), we can state that from this point the full period-adding bifurcation structure does indeed emerge.

In Fig. 3, we present the same $(c, \tilde{n})$-parameter plane, but for larger and smaller values of parameter A: it is $A = 0.8$ in (a) and $A = 0.2$ in (b). In fact, in both figures we still observe the full period-adding structure which is only quantitatively modified. In particular, the border-collision bifurcation boundaries η_L and η_R are defined by $\tilde{n} = 5$ and $\tilde{n} = 5(1+c)$, respectively, in Fig. 3(a), and by $\tilde{n} = 1.25$ and $\tilde{n} = 1.25(1 + c)$, respectively, in Fig. 3(b). One can also notice that the larger A (i.e., the smaller μ), the closer the upper boundary of each periodicity region is to its lower boundary. In fact, at $A = 1$ (or $\mu = 0$), these boundaries coincide. In this case, map F becomes the so-called *circle map* (gap Z is 'closed': $F_R(F_L(\tilde{n})) = F_L(F_R(\tilde{n}))$). For a circle map, irrational rotation is a generic case, so that a generic parameter point corresponds to quasiperiodic trajectories dense in the absorbing interval I (see Avrutin et al. (2019) for details).

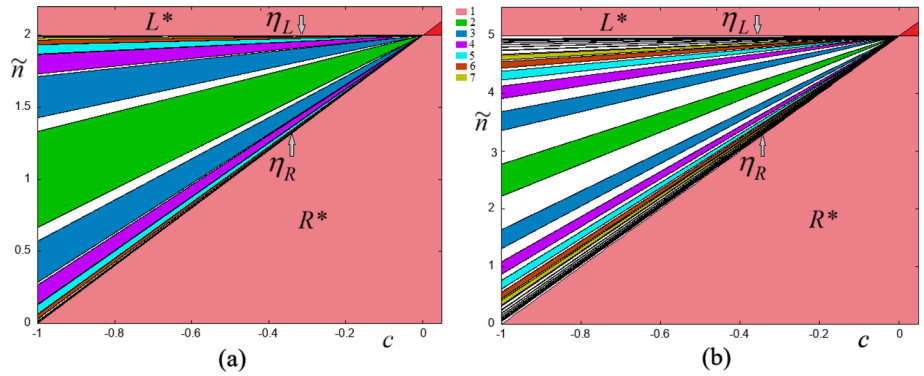

Fig. 4 Border collision bifurcation boundaries of the m-periodicity regions of the first complexity level in the $(c, \tilde{n})$-parameter plane of the map F given in (15) for fixed $A = 0.5$ in **(a)**, and $A = 0.8$ in **(b)**. Here the m-periodicity regions for $m = 1, ..., 7$ are coloured

Let us recall in short how a period-adding structure is organized. It is formed by an infinite number of non-overlapping periodicity regions which are ordered according to the Farey summation rule applied to the rotation numbers of the corresponding cycles. In this way, the basic rule is the following: between any two regions related to cycles with rotation numbers k_1/m_1 and k_2/m_2, such that $|k_1m_2 - k_2m_1| = 1$ (so-called Farey neighbors), there exists a region related to cycles with rotation number $(k_1 + k_2)/(m_1 + m_2)$. For example, between $1/2$- and $1/3$-periodicity regions there is a $2/5$-periodicity region.

To illustrate the period-adding structure, in Fig. 2(b), we show the one-dimensional bifurcation diagram x versus $\tilde{n}$ for fixed $c = -0.5$ and increasing $\tilde{n}, 0.9 < \tilde{n} < 2.1$ (see the vertical arrow in Fig. 2(a)). This parameter path crosses all the periodicity regions constituting the period-adding structure.

The core of a period-adding structure is related to the periodicity regions of attracting cycles having symbolic sequences[8] of the so-called *first complexity level*, LR^{m-1} and RL^{m-1}, $m \geq 2$, with rotation numbers $\rho = 1/m$ and $\rho = (1-m)/m$, respectively. The corresponding cycles are called *basic cycles*. The boundaries of all periodicity regions constituting the period-adding structure are defined by the conditions of the border collision bifurcations of the corresponding cycles. Due to the linearity of the branches of the map F, all these boundaries have analytical representation in terms of parameters. This representation can be obtained iteratively, applying the so-called map replacement technique, starting from the regions of the first complexity level. For the complete set of formulas, we refer to Avrutin et al. (2019) where the map replacement technique is described in detail and the formulas for the boundaries of the higher complexity levels are obtained. In the following, we give the analytical expressions for the first complexity level boundaries. As an example, they are plotted using their analytical expressions in Fig. 4 for $A = 0.5$ in (a) and $A = 0.8$ in (b). The white regions in Fig. 4 are filled with the periodicity regions of higher complexity levels.

[8] An m-cycle $\{x_i\}_{i=0}^{i=m-1}$, $m \geq 2$, can be represented by a symbolic sequence $\sigma = \sigma_0\sigma_1...\sigma_{m-1}$, where $\sigma_i = L$ if $x_i \in L$, and $\sigma_i = R$ if $x_i \in R$.

To give an analytical representation for the boundaries of the periodicity regions associated with the first complexity level, it is convenient to introduce an auxiliary function

$$\psi(A,n)=\begin{cases}\frac{A^n-1}{A-1}, & A\neq 1\\ n, & A=1\end{cases} \tag{20}$$

Consider first a basic cycle $\{x_i\}_{i=0}^{i=m-1}$, $m\geq 2$, with symbolic sequence LR^{m-1}. This cycle can undergo two border collision bifurcations occurring when its first or last point, x_0 or x_{m-1}, collides with the border $x=\tilde{n}$. In terms of parameters, these conditions define two corresponding border collision bifurcation curves denoted $\eta^0_{LR^{m-1}}$ and $\eta^{m-1}_{LR^{m-1}}$:

$$\eta^0_{LR^{m-1}}:\quad \tilde{n}=-\frac{(1+c)\psi(A,m-1)+A^{m-1}}{(A-1)(A^{m-1}+\psi(A,m-1))} \tag{21}$$

$$\eta^{m-1}_{LR^{m-1}}:\quad \tilde{n}=-\frac{(1+c)(\psi(A,m-2)+A^{m-1})+A^{m-2}}{(A-1)(A^{m-2}+A^{m-1}+\psi(A,m-2))} \tag{22}$$

These boundaries converge to the boundary η_R (see 19) as $m\to\infty$. See, for example, the set of periodicity regions located below the 2-periodicity region in Fig. 4.

Now consider a basic cycle $\{x_i\}_{i=0}^{i=m-1}$, $m\geq 2$, with symbolic sequence RL^{m-1}. Similarly, it can undergo two border collision bifurcations that occur when $x_0=\tilde{n}$ or $x_{m-1}=\tilde{n}$. In terms of parameters these conditions define two corresponding border collision bifurcation curves denoted $\eta^0_{RL^{m-1}}$ and $\eta^{m-1}_{RL^{m-1}}$:

$$\eta^0_{RL^{m-1}}:\quad \tilde{n}=-\frac{(1+c)A^{m-1}+\psi(A,m-1)}{(A-1)(A^{m-1}+\psi(A,m-1))} \tag{23}$$

$$\eta^{m-1}_{RL^{m-1}}:\quad \tilde{n}=-\frac{(1+c)A^{m-2}+\psi(A,m-2)+A^{m-1}}{(A-1)(A^{m-2}+A^{m-1}+\psi(A,m-2))} \tag{24}$$

These boundaries converge to the boundary η_L (see 18) as $m\to\infty$. See the set of periodicity regions located above the 2-periodicity region in Fig. 4.

For example, substituting $m=2$ to (21)-(22), we get that for $A\neq 1$, the equations for the border collision bifurcation boundaries η^0_{LR} and η^0_{LR} of the 2-periodicity region are defined as follows:

$$\begin{aligned}\eta^0_{LR}:&\quad \tilde{n}=\tfrac{1+c+A}{1-A^2}\\ \eta^1_{LR}:&\quad \tilde{n}=\tfrac{(1+c)A+1}{1-A^2}\end{aligned} \tag{25}$$

The same equations can be obtained substituting $m=2$ to (23)-(24), because the symbolic sequence of the 2-cycle, which is $LR\equiv RL$, belongs to both families, LR^{m-1} and RL^{m-1}.

The analytical results presented so far are essential to provide a rigorous mathematical foundation for the policy implications of the threshold taxation system discussed in the next section. Before turning to that analysis, we anticipate a few preliminary policy insights that emerge from the graphical investigation of the two-dimensional bifurcations in Figs. 2–4 and that are grounded in the analytical results of this section. In particular, recall that the policy parameter c can take values only in the range $[-1,0]$. At $c=0$, Pigouvian taxation is set to zero, and $R^*=L^*$. Moreover, the map is smooth, upward-sloping, and always converges to the unique equilibrium. It does not matter whether the equilibrium is R^*, when

$\tilde{n} < 1/(1-A)$, or L^*, when $\tilde{n} > 1/(1-A)$, as they are both equal to $1/(1-A)$ and this is the long-run value of environmental damage.

At $c = -1$, and only for $c = -1$, Pigouvian taxation is set at a level such that $R^* = 0$. For $\tilde{n} = 0$, again only for this value, R^* is also an equilibrium of the model, and total abatement is achievable. Hence, the only configuration of the policy parameters $(c, \tilde{n})$ that allows full abatement is $(-1, 0)$.

Moreover, we know that increasing taxation (i.e., reducing c) raises the level of abatement that can be achieved. Nevertheless, from the two-dimensional bifurcation diagrams in Figs. 2–4, we observe that the risk of fluctuations also increases. Indeed, the interval of values of the threshold $\tilde{n}$ for which fluctuations occur, namely (η_L, η_R), with η_L and η_R defined in (18) and (19), respectively, expands as taxation increases (c decreases).

Finally, for $\tilde{n} \geq 1/(1-A)$, there is no risk of fluctuations: the system converges to the unique equilibrium L^*, firms do not perform any abatement, and Pigouvian taxation is ineffective regardless of its level.

4 Economic remarks and policy implications

This section focuses on the policy implications of the global dynamics of the system presented in Section 3. Let us remark that there are two policy tools, summarized by the aggregate parameters c and $\tilde{n}$. Thus, it is crucial to understand the effect of tuning one of these two parameters or both parameters at the same time. Let us recap that increasing the taxation T is equivalent to a reduction of c, while a reduction of the threshold over which the taxation applies is equivalent to a reduction of $\tilde{n}$. Therefore, a more stringent environmental policy is achieved through a reduction in either c or $\tilde{n}$, or in both.

In addition to its stringency, the effectiveness of an environmental policy depends on how it is implemented or design, in particular on the alignment between the Pigovian tax rate c and the threshold $\tilde{n}$ above which the tax applies. Here, we evaluate which strategies for implementing the green policy are effective and under what conditions. Before proceeding with the investigation, let us recall a crucial aspect: regardless of the chosen policy strategy, the long-term level of environmental degradation falls within the range $\left[R^*, L^*\right]$. Here, L^* represents the maximum attainable level of environmental degradation, which is independent of the policy parameters, while R^* denotes the minimum attainable level of environmental degradation, which depends on the policy parameter c associated with environmental taxation. Moreover, for R^* to be an equilibrium of the model, the other policy parameter, namely the threshold $\tilde{n}$, must be sufficiently low.

Aiming to determine which design of the green policy is most effective, we first investigate the effect of tuning a single policy parameter, and then assess the benefits of coordinated tuning of both policy parameters.

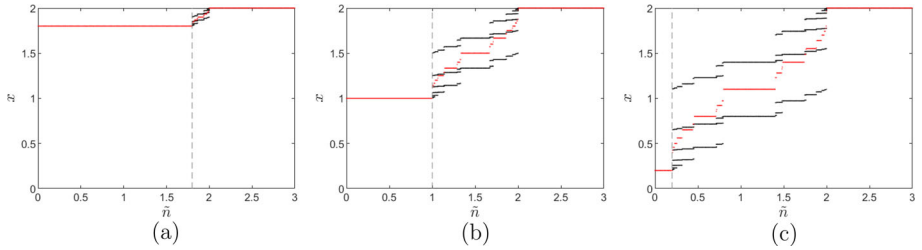

Fig. 5 One-dimensional bifurcation diagram of the map F given in (15) in the $\tilde{n}$-parameter plane for fixed $C = -0.1$ in **(a)**, $C = -0.5$ in **(b)** and $C = -0.9$ in **(c)**. Remaining parameter $A = 0.5$

4.1 A policy strategy based on reducing the no-tax region

A first policy parameter to consider is the reduction of the no-tax region, that is, a reduction of $\tilde{n}$. This policy is effective, as illustrated by the one-dimensional bifurcation diagrams in Fig. 5, where, for each value of the policy parameter $\tilde{n}$, the long-run average value of x is shown in red, while the black points represent the possible values taken by x over time. By starting in the region where L^* is a stable equilibrium (indicating the maximum level of environmental degradation in the long run) and progressively reducing $\tilde{n}$, we observe the emergence of cyclical dynamics. These dynamics result in lower levels of environmental degradation– not just in the average, but across all values. However, if we continue to reduce the no-tax region further, we eventually reach a level where R^* becomes stable. At this stage, the policy strategy loses its effectiveness, as further reductions in the no-tax region do not lead to any changes in the levels of environmental degradation.

4.2 A policy strategy based on an increase of the environmental tax

A key point to emphasize is the impact and effectiveness of taxation, which depends on the level of $\tilde{n}$. As evident from the one-dimensional bifurcation diagrams of Fig. 6(a), due to the presence of a no environmental-tax region $[0, \tilde{n})$, an increase of the taxation (reduction of c) does not have any impact on the equilibrium level of environmental abatement when $L^* < \tilde{n}$. In this scenario, for an increase in the environmental tax to be effective, the policymaker must first reduce the size of the no–environmental-tax region by lowering $\tilde{n}$.

Conversely, the effects of an increase in environmental taxation are more interesting when $R^* > \tilde{n}$. In this case, increasing the environmental taxation (reducing c) reduces the equilibrium value of environmental degradation (R^* reduces). However, a further increase in the taxation may induce fluctuations, that is, entering the parameter region where the map does not admit any equilibrium (that is, $R^* < \tilde{n} < L^*$), see, e.g., the two-dimensional bifurcation diagrams in Figs. 2–4. In this region of the parameter space, the dynamics converge to an attractor–either a periodic cycle or a Cantor set–as proven in the previous section, spanning both the no-environmental-tax and the environmental-tax regions. Consequently, periods of low environmental degradation are followed by periods of high environmental degradation. Under this dynamic regime, it is interesting to examine the average value of environmental degradation. As shown by the one-dimensional bifurcation diagrams in Fig, 6(b)–(c), the

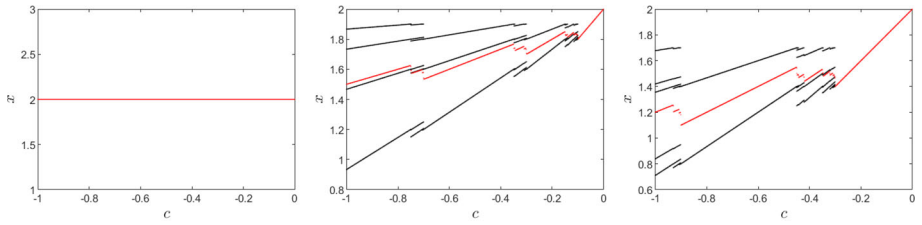

Fig. 6 One-dimensional bifurcation diagram of the map F given in (15) in the c-parameter plane for fixed $\tilde{n} = 2.1$ in **(a)**, $\tilde{n} = 1.8$ in **(b)** and $\tilde{n} = 1.4$ in **(c)**. Remaining parameter $A = 0.5$

average environmental degradation (in red) increases when periodic cycles emerge: higher environmental taxation implies higher average environmental degradation. Further increasing the environmental taxation (further reducing c), this relationship may eventually revert with the environmental degradation, which begins to decrease again.[9] This nonlinear relationship between environmental taxation and environmental degradation underscores the potential risks of implementing a green policy based on a combination of both no-tax and environmental tax regions. This risk can be avoided through a coordinated tuning of the policy parameters, as shown below, where we provide a rule to adjust the threshold in response to a tightening of Pigouvian taxation in order to prevent an increase in average environmental damage.

4.3 A policy strategy based on the tuning of the environmental tax level and the no-tax region

To mitigate the negative effects of increased environmental taxation, a policy suggestion arising from the global analysis presented in Section 3 is to employ a fine-tuning between environmental taxation and the definition of the region without taxation. Specifically, it is recommended to reduce the no-tax region (reduce $\tilde{n}$) when the environmental taxation increases. Starting from a generic set of policy parameter values $\left(c^+, \tilde{n}^+\right)$, the recommendation is to preserve at least the following relation if c is further reduced (which follows from (19)):

$$\tilde{n} = \tilde{n}^+ + \theta \frac{c}{1 - A} \tag{26}$$

with $\theta > 1$. By following this guideline, if we are in the region of the parameter space where the equilibrium R^* exists (equilibrium with low environmental degradation), we remain in this region by increasing the environmental taxation and adjusting, at the same time, the threshold of the no-environmental-tax region. This means that c is reduced and $\tilde{n}$ is reduced as well according to (26). The outcome is a reduction of the levels of environmental degradation, see Fig. 7(a).

[9] The counterintuitive result that an increase in taxation (i.e., a reduction in c) can lead to higher environmental damage can be explained mathematically. Indeed, this occurs only when, by increasing taxation (reducing c), we leave the parameter region where R^* is a stable equilibrium and enter the region where the model generates fluctuations. These fluctuations occur within the range $\left[R^*, L^*\right]$. Hence, crossing the border between these regions inevitably leads to an increase in average environmental damage. However, reducing c produces a second effect: R^* decreases. Which of these two effects prevails determines whether the average damage increases or decreases as c is further reduced. Despite the alternating increases and decreases, numerical simulations confirm an overall trend of decreasing environmental damage as taxation increases.

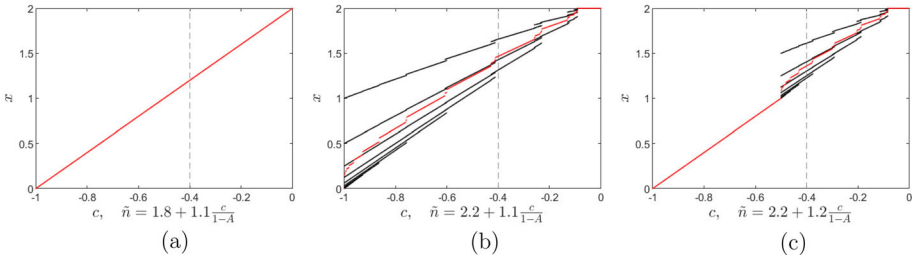

Fig. 7 One-dimensional bifurcation diagram of the map F given in (15) in the c-parameter plane for fixed $\tilde{n} = 1.8 + 1.1\frac{c}{1-A}$ in **(a)**, $\tilde{n} = 2.2 + 1.1\frac{c}{1-A}$ in **(b)** and $\tilde{n} = 2.2 + 1.2\frac{c}{1-A}$ in **(c)**. Remaining parameter $A = 0.5$

Finally, let us consider the region of the parameters space where L^* is the equilibrium of the model. Increasing the environmental taxation and adjusting the threshold of the no-environmental tax region according to the policy rule (26) allow us to enter the region characterized by cycles and (eventually) the region where R^* is the stable equilibrium of the model. This shift requires that θ is sufficiently higher than one, leading to a progressive decrease in the levels of average environmental degradation, as shown in Fig. 7(b)-(c).

An extensive numerical investigation, not reported here for the sake of space, confirms that adjusting the policy parameter according to rule (26) prevents an increase in average environmental damage, as also observable from the one-dimensional bifurcation diagrams in Fig. 7. Overall, we can conclude that this result is supported by the analytical investigation of the global dynamics of the map conducted in the previous section. Indeed, observing an increase in environmental damage in response to higher taxation would require leaving the region of the parameter space where R^* is an equilibrium and entering the region where fluctuations occur. The mathematical analysis of the model's dynamics, particularly with respect to the parameter space, confirms that this cannot happen when the policy is designed following rule (26).

All in all, the policy implications supported by the global dynamics analysed in the previous section, together with the graphical evidence provided by the bifurcation diagrams, can be summarized as follows:

1) By tuning (i.e. reducing) $\tilde{n}$, it is possible to lower the level of environmental damage from L^* (the highest attainable level) to R^* (the lowest attainable level). These two levels do not depend on $\tilde{n}$, and values of environmental degradation below R^* cannot be achieved through this policy instrument alone.
2) By reducing c, that is, by increasing taxation, it is possible to lower the minimum attainable level of environmental damage R^*, while L^* remains independent of c. However, a reduction in c alone does not guarantee that the level R^* can be reached. In such a case, it is also necessary to reduce the threshold level $\tilde{n}$. For sufficiently low values of $\tilde{n}$, the level R^* can always be attained.
3) Given a combination of policy parameters $(c, \tilde{n})$, the following policy prescriptions apply, depending on the observed level of environmental degradation:

   (a) if the observed level is equal to L^*, the policy recommendation is to increase taxation (i.e. reduce c) and adjust $\tilde{n}$ according to rule (26) with a very large value of θ;

(b) if persistent long–run fluctuations are observed, the same policy should be implemented, although a slightly lower value of θ may be adopted;
(c) If the observed level is R^*, further reductions in environmental degradation require a decrease in c and the adoption of rule (26) with $\theta > 1$, although it is sufficient for θ to be only slightly greater than 1.

As a final remark, we underline that the one-dimensional bifurcation diagrams of Figs. 5-7 suggest that the average level of environmental degradation may follow a jump-like process, while displaying a clear trend toward the equilibrium value reached after crossing a bifurcation point as a policy parameter varies. Therefore, the average level of environmental degradation is informative about the direction and the overall effect of the policy tuning implemented by the policymaker. By contrast, the amplitude and the type of fluctuations are less informative about whether a bifurcation point is being approached as a policy parameter is tuned. This is due to the non-smoothness of the model. Indeed, a key feature of such dynamical systems is the possibility of abrupt transitions from equilibrium dynamics to large fluctuations.

5 Conclusions

This paper examines the problem of pollution regulation, focusing on a simple setup where the industry is served by one or a finite number of homogeneous firms. The regulator sets a threshold level of pollution beyond which environmental degradation requires strong regulatory measures. Below this threshold, no particular restrictions are imposed on the industry. Above the threshold level, a Pigouvian pollution tax is imposed, and each firm takes emission abatement measures and pays the tax based on net emissions to the environment. The dynamics of environmental degradation can be modelled through a discontinuous map of the Lorenz type, which has been extensively studied. We present a complete analysis focusing on the most relevant policy parameters, given by the threshold level of environmental degradation that triggers additional measures and the amount of the tax. By maintaining an extremely simple economic structure, we can show analytically the possible dynamics of environmental degradation. Regarding policy implications, we show the existence of a threshold level for the no-tax area that makes taxation ineffective. Moreover, if taxation is increased without proper alignment with the border of the no-tax region, fluctuations can emerge, leading to an increase in the average environmental degradation. Therefore, careful alignment between the border of the no-tax area and the level of taxation is crucial to ensure an effective green policy.

We think that this work can be a first step toward understanding a more complex threshold taxation system. There may be potential room for extensions of the basic model presented here in various dimensions. First of all, it is possible to assume the presence of multiple thresholds of progressive taxation, each of which implies that the model remains unidimensional but with multiple piecewise branches of discontinuity. The economic setup can also be made more general, although this extension seems fairly straightforward. An interesting multidimensional reformulation of the model, on the other hand, may be obtained by incorporating more pollutants into the base model, thus introducing multidimensional thresholds,

that is, a threshold for each pollutant, see Bennett et al. (2008). We feel we should leave such extensions to future work on the subject.

Acknowledgements The authors are grateful to the journal editors and the two anonymous referees for their insightful comments and constructive suggestions, which greatly improved the quality of the manuscript. The work of Fabio Lamantia is funded by the PRIN 2022 under the Italian Ministry of University and Research (MUR) Prot. 2022YMLS4T – TEC – Tax Evasion and Corruption: theoretical models and empirical studies. A quantitative-based approach for the Italian case. The work of Davide Radi and Iryna Sushko has been funded by the European Union - Next Generation EU, Missione 4: "Education and Research" - Componente 2: "From research to business", through PRIN 2022 under the Italian Ministry of University and Research (MUR). Project: 2022JRY7EF - Qnt4Green - Quantitative Approaches for Green Bond Market: Risk Assessment, Agency Problems and Policy Incentives - CUP: J53D23004700008. Davide Radi thank the European Union (REFRESH Project-Research Excellence for Region Sustainability and High-Tech Industries of the European Just Transition Fund, Grant CZ.10.03.01/00/22 003/000004). This paper was written with the financial support of the Student Grant Competition at the Faculty of Economics of the VSB - Technical University of Ostrava within the project SP2026/003. Davide Radi thanks the Gruppo Nazionale di Fisica Matematica GNFM-INdAM for financial support.

Funding Open access funding provided by Università Cattolica del Sacro Cuore within the CRUI-CARE Agreement.

Declarations

Conflicts of Interest All authors declare that they have no conflicts of interest.

References

Avrutin, V., Gardini, L., Sushko, I., & Tramontana, F. (2019). *Discontinuous Piecewise-Smooth One-Dimensional Maps*. Singapore: World Scientific.

Avrutin, V., Schanz, M., & Gardini, L. (2010). Calculation of bifurcation curves by map replacement. *International Journal of Bifurcation & Chaos, 20*(10), 3105–3135.

Bennett, E. M., Carpenter, S. R., & Cardille, J. A. (2008). Estimating the risk of exceeding thresholds in environmental systems. *Water, Air & Soil Pollution, 191*, 131–138.

Berry, D., & Mestel, B. (1991). Wandering interval for lorenz maps with bounded nonlinearity. *Bulletin of the London Mathematical Society, 23*, 183–189.

Buccella, D., Fanti, L., & Gori, L. (2021). To abate, or not to abate? a strategic approach on green production in cournot and bertrand duopolies. *Energy Economics, 96*, Article 105164.

Buccella, D., Fanti, L., & Gori, L. (2024). Environmental policies in a polluting duopoly: a simple comparison. *Italian Economic Journal*, 1–26.

Buccella, D., Fanti, L., Gori, L., & Sodini, M. (2024). The abatement game in a dynamic oligopoly: social welfare versus profits. *Annals of Operations Research, 337*, 1037–1065.

Carlsson, F. (2000). Environmental taxation and strategic commitment in duopoly models. *Environmental and Resource Economics, 15*, 243–256.

Chidiac, S., El Najjar, P., El Rayess, Y., Ouaini, N., & El Azzi, D. (2023). A comprehensive review of water quality indices (wqis): history, models, attempts and perspectives. *Reviews in Environmental Science and Bio/Technology, 22*, 349–395.

Feng, L., Shi, Y., Yang, Z., Lam, J. F. I., Lin, S., Zhan, J., & Chen, H. (2025). Dynamic correlation of environmental regulation, technological innovation, and corporate carbon emissions: Empirical evidence from china listed companies. *Scientific Reports, 15*, 8433.

Gardini, L., Avrutin, V., & Sushko, I. (2014). Codimension-2 border collision bifurcations in one-dimensional discontinuous piecewise smooth maps. *International Journal of Bifurcation & Chaos, 24*(2), 1450024.

Gardini, L., Tramontana, F., Avrutin, V., & Schanz, M. (2010). Border collision bifurcations in $1d\ pwl$ map and Leonov's approach. *International Journal of Bifurcation & Chaos, 20*(10), 3085–3104.

He, L., Yuan, B., Bian, J., & Lai, K. K. (2023). Differential game theoretic analysis of the dynamic emission abatement in low-carbon supply chains. *Annals of Operations Research, 324*, 355–393.

Homburg, A. J. (1996). *Global Aspects of Homoclinic Bifurcations of Vector Fields*. Berlin: Springer-Verlag.

Jørgensen, S., Martín-Herrán, G., & Zaccour, G. (2010). Dynamic games in the economics and management of pollution. *Environmental Modeling & Assessment, 15*, 433–467.

Keener, J. P. (1980). Chaotic behavior in piecewise continuous difference equations. *Transactions of the American Mathematical Society, 216*, 589–604.

Ma, L., Ma, S., Tang, Q., Sun, M., Yan, H., Yuan, X., et al. (2024). Environmental regulation effect on the different technology innovation-based: an empirical analysis. *PLoS One, 19*(1), Article e0296008.

Manta, A. G., Doran, N. M., Bădîrcea, R. M., Badareu, G., & Tăran, A. M. (2023). Does the implementation of a pigouvian tax be considered an effective approach to address climate change mitigation? *Economic Analysis and Policy, 80*, 1719–1731.

Marsiglio, S., & Tolotti, M. (2024). Complexity in low-carbon transitions: Uncertainty and policy implications. *Energy Economics, 138*, Article 107803.

Nusse, H. E., & Yorke, J. A. (1992). Border-collision bifurcations including period two to period three for piecewise smooth systems. *Physica D: Nonlinear Phenomena, 57*, 39–57.

Rand, D. (1978). Exotic phenomena in games and duopoly models. *Journal of Mathematical Economics, 5*(2), 173–184.

Segerson, K. (1988). Uncertainty and incentives for nonpoint pollution control. *Journal of Environmental Economics and Management, 15*(1), 87–98.

La Torre, D., Marsiglio, S., & Privileggi, F. (2025). A game of transboundary pollution under endogenous ecological uncertainty. *Environmental and Resource Economics, 88*, 2885–2906.

Ulph, A. (1996). Environmental policy and international trade when governments and producers act strategically. *Journal of Environmental Economics and Management, 30*(3), 265–281.

van der Ploeg, F., & de Zeeuw, A. J. (1992). International aspects of pollution control. *Environmental and Resource Economics, 2*, 117–139.